Adjustable ac Capacitor for a Single-Phase Induction Motor

Eduard Muljadi, *Member, IEEE,* Yifan Zhao, Tian-Hua Liu, *Member, IEEE,* and Thomas A. Lipo, *Fellow, IEEE*

Abstract— **The most common practice for starting a single-phase induction machine (SPIM) is to install a starting capacitor in series with the auxiliary winding. In some applications, two capacitors are used. One is used during the starting period to help create the starting torque. The other one is used during the running condition to improve efficiency. This paper discusses the possibility of using an electronic switch in parallel with the running capacitor, thereby providing the equivalent of a starting capacitor. The capacitor is shorted during each cycle to vary the effective size of the ac capacitor. By using this method, only one capacitor is used for both the starting and running condition, and a similar starting performance can be obtained when compared with the conventional method using two capacitors.**

I. Introduction

THE SINGLE-PHASE induction machine (SPIM) is the most widely used type of ac machine in the world. Despite all its merits, the SPIM has disadvantages when it comes to realizing the beauty of the smoothly rotating flux found in three-phase machines. One of the major problems associated with the design of a SPIM is that unlike a three-phase winding system, a single phase does not produce a rotating magnetic field. Instead, the magnetic field produced by a single phase remains stationary in position and pulsates with time. Since there is no net rotating magnetic field, single-phase induction motors cannot start without modification. The most common type of starting aid used to start a SPIM is the starting capacitor installed in series with the auxiliary winding. Typical applications for such motors are compressors, pumps, air conditioners, and other pieces of equipment that must start under load.

The function of the capacitor is to realize another phase from the supply source to feed a second, auxiliary winding so that the motor can operate as a two-phase machine. For this purpose, the capacitor size must be carefully determined according to the terminal impedance of the auxiliary winding. Unfortunately, this impedance changes dramatically from the starting to the running condition. Hence, it is not practical to use only one fixed value capacitor for both starting and running. If both the largest starting torque and best running conditions are needed, at least two capacitors must be used with the auxiliary winding. Motors with two capacitors are called capacitor-start, capacitor-run, or two-value capacitor motors. The larger capacitor is present in the circuit only during starting when it ensures that the currents in the main and auxiliary windings are roughly balanced, yielding a relatively high starting torque. When the motor runs up to speed, the centrifugal switch opens, and the permanent capacitor is left by itself in the auxiliary winding circuit. The permanent capacitor is just large enough to balance the currents at normal motor loads; therefore, the motor again operates efficiently with good power factor. The permanent capacitor in such a motor is typically about 10 to 20% of the size of the starting capacitor that, together with the centrifugal switch, accounts for a considerable portion of the cost of the system.

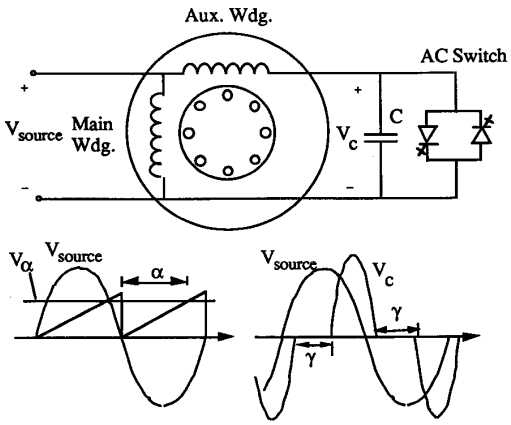

Fig. 1. Circuit layout of the proposed system and circuit operation.

In this paper, it is proposed that the centrifugal switch and starting capacitor be eliminated and a switched capacitor used, as shown in Fig. 1. In this case, the system consists of three major elements: the induction machine, the running capacitor, and an inverse/parallel set of bidirectional voltage blocking switches (e.g., reverse blocking GTO's). The main winding of the SPIM is directly connected to the supply mains. It is shown that the apparent capacitance of the running capacitor can be made larger than its actual value if the capacitor is shorted periodically. Thus, by operating the switch on and off regularly during each cycle and by changing the length of the shorting interval γ, the effective capacitance of the capacitor

Paper IPCSD 92-35, approved by the Industrial Drives Committee of the IEEE Industry Applications Society for presentation at the 1991 Industry Applications Society Annual Meeting, Dearborn, MI, September 28–October 4. This work was supported by the member companies of the Wisconsin Electric Machines and Power Electronics Consortium. Manuscript released for publication August 17, 1992.

E. Muljadi is with the National Renewable Energy Laboratory, Golden, CO 80401.

Y. Zhao and T. A. Lipo are with the Department of Electrical and Computer Engineering, University of Wisconsin, Madison, WI 53706-1691.

T.-H. Liu is with the Department of Electrical Engineering, National Taiwan Institute of Technology, Taipei, Taiwan, R.O.C.

IEEE Log Number 9208798.

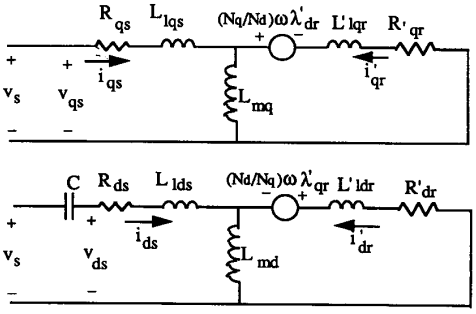

Fig. 2. Single-phase induction machine equivalent circuit.

can be enlarged and adjusted to an optimal value to realize the maximum possible acceleration torque for any rotor speed during run-up from standstill. By using this method, only one capacitor is used for both starting and running conditions.

II. Motor D-Q Model

Before discussing the control strategy of the system, it is necessary to first investigate the general characteristics of the SPIM running at the various speeds with varying capacitor values.

For purposes of analysis, the capacitor-run single-phase induction machine can be considered to be an unsymmetrical two-phase induction machine. The analysis of such machines can be conveniently handled by the normal d-q model approach used for three-phase machines. The details of the derivation of the d-q model as applied to unsymmetrical two-phase induction machines are described in [1]. The resulting equivalent circuit representing the SPIM is shown in Fig. 2, and the machine model can be expressed in matrix form by the following equations [1]:

$$v_{qs}^{s} = V_s$$
$$v_{ds}^{s} = V_s - \frac{1}{C}\int i_{ds}^{s}\, dt. \tag{2}$$

The definitions of the terms in (1), which is shown at the bottom of this page, and (2) are as follows:

q-axis Parameters:

R_{qs} stator main winding resistance
X_{mq} $= qs$-axis magnetizing reactance
X_{mq} $= (N_q/N_r) \cdot X_{mr}$

where N_q is the number of turns of the stator main winding, N_r is the equivalent number of turns of the corresponding rotor winding, and X_{mr} is the mutual reactance between the two windings.

X_{qs} is the qs-axis stator self-reactance, and $X_{qs} = X_{lqs} + X_{mq}$, where X_{lqs} is the stator main winding leakage reactance.

$R_{qr}^{'}$ rotor winding resistance referred to stator main winding
$X_{qr}^{'}$ rotor self-reactance referred to stator main winding
$X_{qr}^{'} = X_{lqr}^{'} + X_{mq}$

where $X_{lqr}^{'}$ is the rotor leakage reactance referred to the stator main winding.

d-axis Parameters:

R_{ds} stator auxiliary winding resistance
X_{md} ds-axis magnetizing reactance
$X_{md} = (N_d/N_r) \cdot X_{ar}$

where N_d is the number of turns of the stator auxiliary winding, X_{ar} is the amplitude of the mutual reactance between the stator auxiliary winding and the rotor windings.

X_{ds} is the ds-axis stator self-reactance, and $X_{ds} = X_{lds} + X_{md}$, where X_{lds} is the stator auxiliary winding leakage reactance.

$R_{dr}^{'}$ rotor winding resistance referred to stator auxiliary winding
$X_{dr}^{'}$ rotor self-reactance referred to stator auxiliary winding
$X_{dr}^{'} = X_{ldr}^{'} + X_{md}$

where $X_{ldr}^{'}$ is the rotor leakage reactance referred to the stator auxiliary winding.

Other parameters and variables include the following:

v_{ds}^{s}, v_{qs}^{s} ds-axis and qs-axis stator voltages
i_{ds}^{s}, i_{qs}^{s} ds-axis, qs-axis stator currents
$i_{dr}^{'s}$, $i_{qr}^{'s}$ rotor currents referred to the stator ds- and qs-axes
V_s supply voltage
p differential operator d/dt
ω_b base angular velocity
ω_r rotor angular velocity.

The instantaneous electromagnetic torque can be expressed as

$$T_e = \frac{P}{2}\frac{N_d}{N_q}\frac{X_{mq}}{\omega_b}(i_{qs}^{s} i_{dr}^{'s} - i_{ds}^{s} i_{qr}^{'s}) \tag{3}$$

where P is the number of poles of the machine.

III. Steady-State Control Principle

From the resulting equations, it is possible to generate a contour graph of torque as function of slip and the capacitance as shown in Fig. 3(a). As can be seen from this graph, the significant characteristic is that the starting torque reaches its maximum value at a certain capacitance when the motor is at standstill. After this point, the capacitance related to the maximum torque begins to decrease as the speed increases.

$$[v_{qs}^{s}\ v_{ds}^{s}\ 0\ 0]T = \begin{bmatrix} R_{qs} + \frac{p}{\omega_b}X_{qs} & 0 & \frac{p}{\omega_b}X_{mq} & 0 \\ 0 & R_{ds} + \frac{p}{\omega_b}X_{ds} & 0 & \frac{p}{\omega_b}X_{md} \\ \frac{p}{\omega_b}X_{mq} & -\frac{N_q}{N_d}\cdot\frac{\omega_r}{\omega_b}X_{md} & R_{qr}^{'} + \frac{p}{\omega_b}X_{qr}^{'} & -\frac{N_q}{N_d}\cdot\frac{\omega_r}{\omega_b}X_{dr}^{'} \\ \frac{N_d}{N_q}\cdot\frac{\omega_r}{\omega_b}X_{mq} & \frac{p}{\omega_b}X_{md} & \frac{N_d}{N_q}\cdot\frac{\omega_r}{\omega_b}X_{qr}^{'} & R_{dr}^{'} + \frac{p}{\omega_b}X_{dr}^{'} \end{bmatrix} \cdot [i_{qs}^{s}\ i_{ds}^{s}\ i_{qr}^{'s}\ i_{dr}^{'s}]T \tag{1}$$

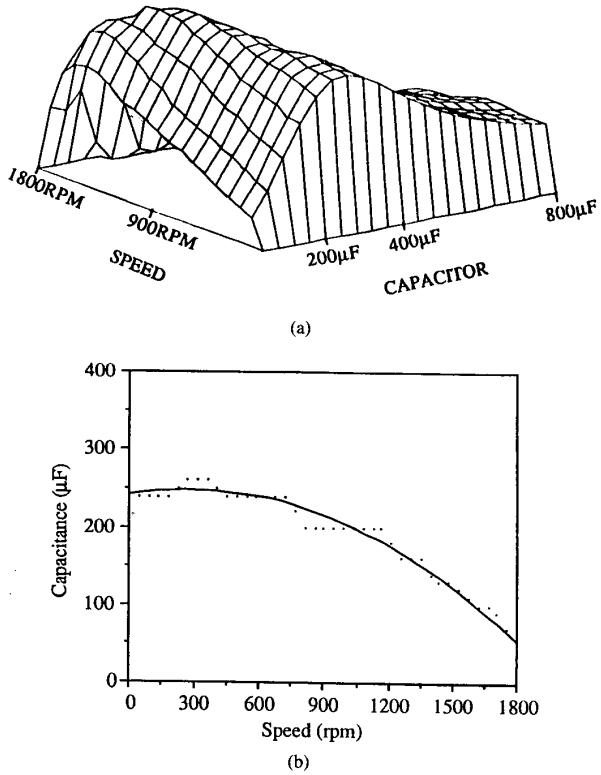

Fig. 3. (a) Contour graph of torque as a function of capacitor size and motor speed; (b) optimal starting curve of capacitance as a function of motor speed.

The optimal starting curve of capacitance as a function of speed can be obtained from Fig. 3(a) by projecting the path of the peak torque given on the contour graph onto the capacitance-speed plane as shown in Fig. 3(b). The dotted lines in Fig. 3(b) indicate the points projected in this manner from Fig. 3(a). Because of the inherent round-off difficulties in this process, the points are somewhat scattered. However, the solid line in Fig. 3(b) shows the smoothed result.

Based on the torque variation available from the contour graph of Fig. 3, it is clear that one can choose an optimal path to control the capacitance to achieve an optimized starting performance. However, due to the difficulty in realizing an adjustable capacitor and the need for a speed sensor for realizing optimal starting, the most common practice has been to choose the starting capacitor to satisfy the zero-speed torque requirements and to keep the capacitance constant from zero speed to a speed near rated speed at which point the centrifugal switch opens. It can be seen from Fig. 3 that the starting performance resulting from the use of a fixed starting capacitor is far from optimal. Another problem raised from this approach is the unavoidable use of a mechanical centrifugal switch.

IV. Switched-Capacitor Start Principle

The concept of switched capacitor provides an effective means to solve the problems associated with the need for a variable capacitor. The switched capacitor consists of an ac capacitor in parallel with an electronic switch, and the

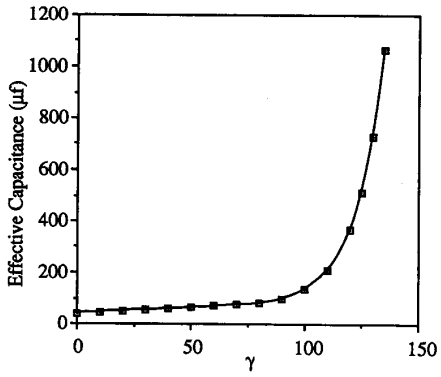

Fig. 4. Effective size of a 40-μF ac capacitor operating as switched capacitor versus control angle γ.

switch is allowed to periodically turn on and off during each cycle. When the switch is open, current flows through the capacitor, which is placed in series with the auxiliary winding. The current bypasses the capacitor when the switch is closed. The switch is closed at the instant the voltage across the capacitor reaches zero. Thus, a zero-voltage switching operation is performed, and the switch remains closed until it is opened by the command signal. The effective value of the ac capacitor can be adjusted if the magnitude of the fundamental component of the voltage across the switch is adjusted independent of the current flowing through it. Hence, by shorting the switch periodically, the fundamental component of the voltage across the capacitor appears to be lower than the case without a shorting period so that the effective size of the capacitor appears to be larger than its actual size. As the shorting interval γ reaches π rad, the effective size of the capacitor approaches infinity because the switch is closed during entire cycle. Fig. 4 shows a calculated result showing the effective size of a 40-μF running capacitor being operated as a switched capacitor for a given set of machine parameters.

Although one can control the angle γ to adjust the effective capacitance, the switched capacitor can also be implemented by controling the firing angle α of the switch. The firing angle α is controlled directly by a sawtooth waveform generator that has a frequency twice the frequency of the voltage supply and is synchronized to the supply. The sawtooth waveform is then compared with a dc bias voltage V_α, which represents the firing angle, and the switch is opened when the sawtooth voltage is equal to the V_α. The switch is closed at the zero crossing point of the capacitor voltage. The overall concept is again illustrated by Fig. 1. In this case, the effective size of the capacitor is determined both by the angle α and the instant of the capacitor voltage zero crossing. However, since the machine impedance changes when the speed changes, the zero crossing point will also change. Hence, the effective size of the capacitor will not be maintained constant even if α is maintained constant. Fig. 5 shows a simulation result demonstrating the influence of the speed changes on the shorting angle γ. The firing angle α in Fig. 5 is the same. However, in Fig. 5(a), the machine is in the standstill condition, whereas in Fig. 5(b), the machine

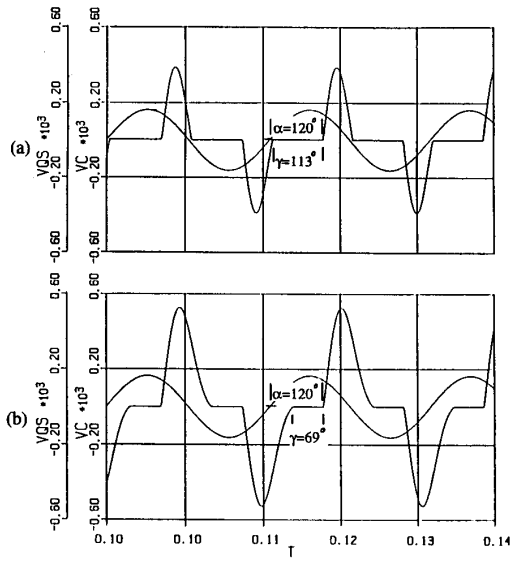

Fig. 5. Influence of speed change on shorting interval γ: (a) Speed $n = 0.0$ r/min, $\alpha = 120°$, $\gamma = 113°$; (b) $n = 1700$ r/min, $\alpha = 120°$, $\gamma = 69°$.

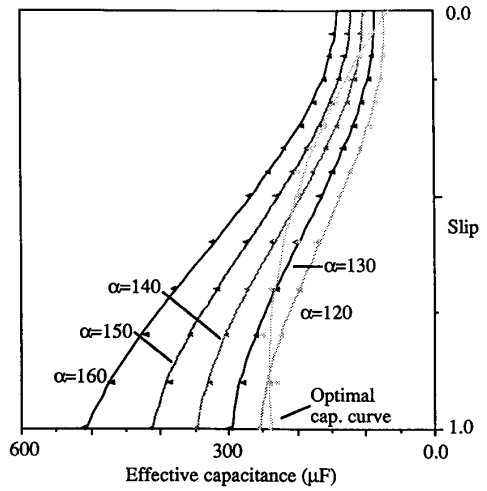

Fig. 6. Relationship between effective capacitance and speed.

is running at 1700 r/min. It can be seen that the value of γ in Fig. 5(a) is much larger than that of Fig. 5(b) so that the effective capacitance corresponding to Fig. 5(a) will appear to be larger as well.

Fig. 6 shows the change of the effective capacitance versus speed for various values of the control angle α. The optimal path in Fig. 3 is again drawn in Fig. 6. The advantage of using firing angle control method can be immediately found from Fig. 6. In particular, the inherent changing nature of the motor

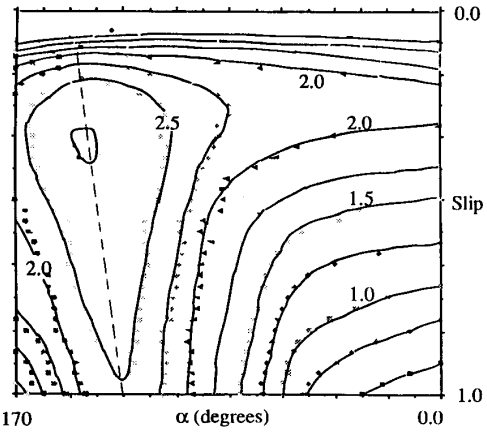

Fig. 7. Contour graph of torque (in pu value) as a function of speed and control angle α.

impedance during starting, which is the major reason for using two capacitors in the conventional SPIM design, becomes an advantage when a switched capacitor and firing angle control method is used to start the motor. As a result of the speed change, the effective size of the capacitor automatically becomes increasingly smaller as the motor speed increases, thereby making the effective capacitor curve come closer to the optimal path compared with the use of a fixed value starting capacitor.

To provide another viewpoint concerning motor torque production with a controled capacitor, a contour graph of the motor torque as a function of speed and firing angle has been calculated and is plotted in Fig. 7. As can be expected, the optimal path (dashed line) in Fig. 7 is very close to a constant α line. Thus, it can be expected that a satisfactory starting performance can be obtained by using a switched capacitor and constant α control.

V. Control Strategy

It is evident that the starting performance can be further improved if α is adjusted to always follow an optimal path. However, the benefit obtained will not be as significant as that obtained by the constant α control, compared with the fixed capacitor value, and the inevitable tradeoff is that a speed sensor must then be used. In this paper, the switched capacitor is simply controlled under constant α control. Fig. 8 shows the block diagram of the control circuit that was implemented in hardware. In this control, the main winding current is used to terminate the switching operation on the capacitor when the motor reaches nominal speed. Because of the orthogonality of the two windings in the SPIM, the switching action in the auxiliary winding circuit has very little influence on the amplitude of main winding current, and sensitivity of the constant α controler to the changes in speed greatly increases when the machine is near the running condition. Hence, the α controler is simply disabled at this point. It should be pointed out that a low-cost current sensor can be used due to its simple function in the circuit.

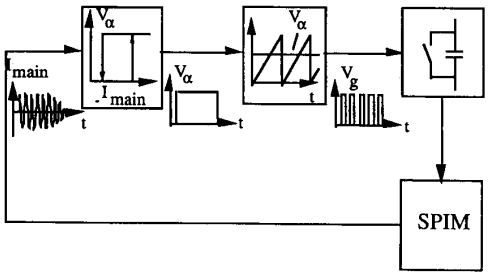

Fig. 8. Control circuit block diagram.

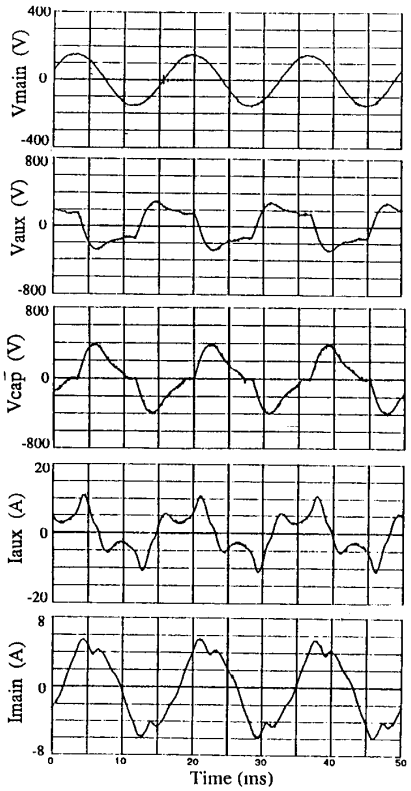

Fig. 9. Typical voltage and current waveforms (α = 100°, load torque T_1 = 4.0 N.m, speed n = 1725 r/min): (a) Main winding voltage; (b) auxiliary winding voltage; (c) capacitor voltage; (d) auxiliary winding current; (e) main winding current.

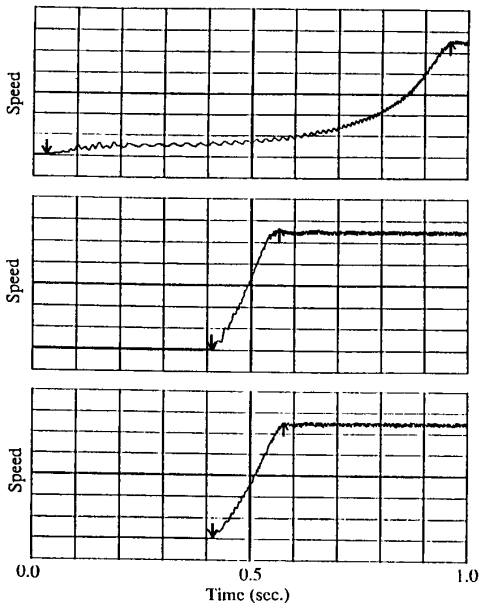

Fig. 10. Acceleration of SPIM under 0.15 load torque: (a) Using installed running capacitor (40 μF); (b) using installed starting capacitor (250 μF); (c) using switched running capacitor (40 μF).

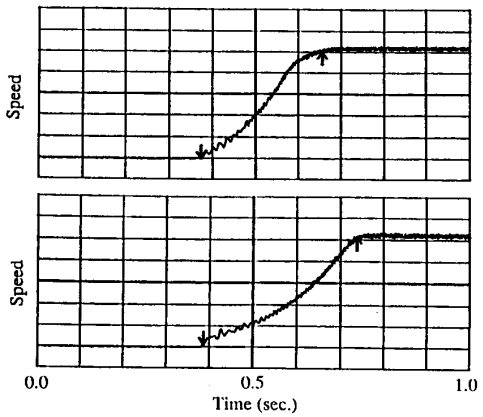

Fig. 11. Acceleration of SPIM under rated load torque: (a) Using installed starting capacitor (250 μF); (b) using switched running capacitor (40 μF).

VI. Experimental Results

The voltage applied to the auxiliary winding is the result of the supply voltage and the capacitor voltage. The current entering the auxiliary winding, which can also be considered as the current passing through the effective capacitor (the switch and the running capacitor), is the sum of capacitor current and the switch current. The capacitor voltage and the voltage across the auxiliary winding are not smooth sinusoidal due to the existence of switching action on the capacitor. The switching applied to the capacitor generates a resonance between the inductance of SPIM and the capacitor. As a result, the current entering the auxiliary winding is also not a smooth sinusoidal. Fig. 9 shows the typical waveforms of the voltages and the currents. It can be seen that if only the fundamental components are considered, the voltage across the capacitor lags the auxiliary current by 90°. It is also shown that the auxiliary winding voltage is shifted by approximately 90° with respect to the main winding voltage V_s, and consequently, the auxiliary winding current is similarly shifted with respect to the main winding current. It is apparent that substantial loss-producing harmonics are induced in the motor. However, since this condition persists only during the brief acceleration period, such additional losses can be considered as having a negligible effect on the thermal design and efficiency of the motor.

Acceleration of a SPIM utilizing control of V_α is shown in Figs. 10 and 11. For the parameters of the SPIM summarized in the Appendix, the constant value of α was selected at 130°.

For the purpose of comparison, the motor was started with its rated running capacitor (40 μF), its rated starting capacitor (250 μF), and then with a switched 40-μF running capacitor under a light-load torque condition. The light-load condition was chosen to enable the motor to start when utilizing the relatively small running capacitor. Fig. 10 shows the acceleration of the SPIM for the three cases. It can be seen that the use of the running capacitor for starting produces only a very small accelerating torque. However, when the capacitor is switched in accordance with the principles proposed in this paper, the time to accelerate to rated speed approaches the time achieved by using the optimum capacitor very closely. The fact that the start time required by the switched starting capacitor is slightly greater than when using the starting capacitor can be attributed to the additional losses produced by switching the running capacitor. Fig. 11 shows a comparison of starting performance using the optimum 250-μF capacitor versus the switched 40-μF running capacitor when starting under rated load. Although an increase in starting time when using the switched running capacitor is now more apparent, it is still very close to the case of the optimum capacitor. When the running capacitor is used without switching, it was incapable of starting under more than 0.2-pu load.

It should be noted in passing that for the motor tested, the starting capacitor actually supplied with the tested motor was 506 μF rather than the optimum value of 250 μF used for these tests. Hence, starting performance using the switched running capacitor actually showed a marked improvement when compared with the installed running capacitor rather than the optimally calculated 250 μF.

VII. Conclusion

This paper has presented a new scheme for starting a single-phase induction motor. By periodically and synchronously shorting the running capacitor with a solid-state switch, the need for a separate starting capacitor and start/run switch can be eliminated. Since the starting capacitor can now be dynamically varied, the optimum capacitor value can be selected for any rotor speed. However, it was shown that by simply controling as constant the switch turn-off instant with respect to the source voltage zero crossing, good starting performance can be obtained with a minimum of complexity. Since the starting switch is one of the most failure prone components of a typical capacitor-run single-phase motor, due to arcing of the mechanical contacts, elimination of this device is expected to significantly improve the reliability of such machines.

Appendix

Motor Nameplate Data

Hz	60	hp	1
r/min	1725	volt	115/230
fla	8.6/4.3	sf	1.15.

Motor Parameters

$R_{qs} = 3.52\ \Omega$ $R_{ds} = 0.785\ \Omega$

$R'_{qr} = 4.746\ \Omega$ $R'_{dr} = 1.614\ \Omega$

$L_{lqs} = 0.00902$ H $L_{lds} = 0.00327$ H

$L'_{lqr} = 0.00876$ H $L'_{ldr} = 0.00318$ H

$L_{mq} = 0.199$ H $L_{md} = 0.0722$ H

$N_q/N_d = 1.66$

Running capacitor = 40 μF

Starting capacitor = 506 μF (Measured value of factory supplied starting capacitor).

References

[1] P. C. Krause and C. H. Thomas, "Simulation of unsymmetrical 2-phase induction machines," *IEEE Trans. Power App. Syst.*, vol. PAS-84, no. 11, pp. 1025–1037, Nov. 1965.

[2] P. C. Krause, *Analysis of Electric Machinery.* New York: McGraw-Hill, 1986.

[3] Fitzgerald, Kingsley, and Umans, *Electric Machinery.* New York: McGraw-Hill, 1984.

Eduard Muljadi (M'83) received the B.S.E.E. degree from Surabaya Institute of Technology in 1981, M.S. and Ph.D. degrees from the University of Wisconsin, Madison, in 1984 and 1987, respectively.

From 1988 to 1992, he taught at the Department of Electrical and Computer Engineering at California State University, Fresno, CA, as an associate professor. Since June 1992, he joined the National Renewable Energy Laboratory (NREL), Golden, CO. His current research interests are in the fields of electric machine drives and power electronics.

Yifan Zhao was born in Zheng-zhou, China. He received the B.S. degree from Jiaozuo Institute of Mining, China, in 1982 and the M.S. degree from China University of Mining and Technology in 1985, both in electrical engineering. He is currently a Ph.D. student at the Department of Electrical and Computer Engineering, University of Wisconsin-Madison.

He was with the Industrial Automation Department, China University of Mining and Technology, from 1985 to 1990. His research interests include microprocessor control systems, electric machines and drives, and power electronic circuits.

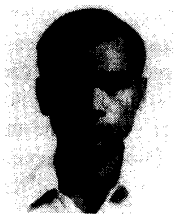

Tian-Hua Liu (S'85–M'89) was born in Tao Yuan, Taiwan, Republic of China, on November 26, 1953. He received the B.S., M.S., and Ph.D. degrees from National Taiwan Institute of Technology, Taipei, Taiwan, in 1980, 1982, and 1989, respectively, all in electrical engineering.

From 1984 to July 1989, he was an Instructor in the Department of Electrical Engineering, National Taiwan Institute of Technology. He was a Visiting Professor in the Department of Electrical and Computer Engineering of the University of Wisconsin-Madison from 1990 to 1991. Since August 1989, he has been an Associate Professor in the Department of Electrical Engineering, National Taiwan Institute of Technology. His research interests include motor controls, power electronics, and microprocessor-based control systems.

Thomas A. Lipo (F'87) received the B.E.E. and M.S.E.E. degrees from Marquette University, Milwaukee, WI, in 1962 and 1964, respectively, and the Ph.D. degree in electrical engineering from the University of Wisconsin in 1968. He was an NRC Postdoctural Fellow at the University of Manchester Institute of Science and Technology, Manchester, England, from 1968 to 1969.

From 1969 to 1979, he was an Electrical Engineer in the Power Electronics Laboratory of Corporate Research and Development of hte General Electric Company, Schenectady, NY. He became Professor of Electrical Engineering at Purdue University, West Lafayette, IN, in 1979 and later joined the University of Wisconsin, Madison, in the same capacity. He has been involved in the research of power electronics and ac drives for over 25 years.

Dr. Lipo has received 11 IEEE prize paper awards including corecipient of the Best Paper Award in IEEE TRANSACTIONS ON INDUSTRY APPLICATIONS for 1984. In 1986, he received the Outstanding Achievement Award from the IEEE Industry Applications Society for his contributions to the field of ac drives.